DOI: 10.24996/ijs.2020.61.4.21

ISSN: 0067-2904

The Numerical Approximation of the Bioheat Equation of Space-Fractional Type Using Shifted Fractional Legendre Polynomials

Firas A. Al-Saadawi[1*], Hameeda Oda Al-Humedi[2]
[1]Department Mathematics, Open Educational College in Basra, Basrah, Iraq.
[2]Department Mathematics, College of Education for Pure Sciences, Basrah University, Basrah, Iraq

Received: 17/8/ 2019 Accepted: 30/9/2019

Abstract

The aim of this paper is to employ the fractional shifted Legendre polynomials (FSLPs) in the matrix form to approximate the fractional derivatives and find the numerical solutions of the one-dimensional space-fractional bioheat equation (S-FBHE). The Caputo formula was utilized to approximate the fractional derivative. The proposed methodology applied for two examples showed its usefulness and efficiency. The numerical results showed that the utilized technique is very efficacious with high accuracy and good convergence.

Keywords: Collocation method, Space-Fractional bioheat equation, Fractional shifted Legendre polynomials, Numerical accuracy.

متعددات حدود ليجندر الكسورية التقريب العددي لحل معادلة الكسوريه بأستخدام *Bioheat*

فراس عامر السعداوي[1]*، حميده عوده الحميدي[2]
[1]قسم الرياضيات، الكلية التربوية المفتوحة في البصرة، البصرة، العراق
[2]قسم الرياضيات، كلية التربية للعلوم الصرفة، جامعة البصرة، البصرة، العراق

الخلاصة

الهدف من هذا البحث هو توظيف متعددات الحدود ليجندر الكسورية (FSLPs) بالشكل المصفوفي لتقريب المشتقات الكسورية لإيجاد الحلول العددية لمعادلة bioheat الكسورية أحادية البعد (S–FBHE) . أستخدمنا صيغة Caputo لتقريب المشتقة الكسورية . تبين المنهجية المقترحة المطبقة على مثالين فائدتها وكفائتها. تظهر النتائج العددية أن التقنية المستخدمة فعالة للغاية، وتعطي دقة عالية وتقاربًا جيدًا.

1. Introduction

Many problems in various fields can be successfully modeled by the ordinary, partial or fractional differential equations. Fields of application include, for example, biomedical engineering, physics, viscoelasticity, biology, and fluid mechanics ,etc. In many cases, finding the exact solutions for these equations is difficult or impossible. Therefore, researchers used approximate or numerical solution methods [1-5].

The fractional calculus is utilized to improve the modeling accuracy of many phenomena in natural sciences. The most important merit of utilizing fractional differential equations is their non-local

*Email: firasamer519@yahoo.com

property. This means that the next case of a system depends not only upon its current case but also upon all of the non-local properties. These are more factual and represent an important cause of making the fractional calculus more popular. In medicine, the fractional order model may be the proper one for modeling of dynamic systems [6].

Heat distribution in biological tissues is typically expressed as a bioheat equation. It involves thermic conduction, perfusion of blood, convection and metabolic temperature generation in human tissues [7]. The pioneering work of Pennes in 1948 was the cornerstone of the mathematical modeling of temperature distribution in tissues, with the bioheat equation still being extensively used [8]. The temperature distribution in the skin tissue is very important for medical application such as skin cancer, skin burns ,etc [9]. The fractional bioheat model has attracted the focus of the researchers and it contributes to a significant rate of the ongoing research [10-18].

In this work, we introduce a numerical approach for solving the one-dimensional S-FBHE based on FSLPs.

2. Governing Equation

The space-fractional version of the one-dimensional unsteady state of bioheat equation can be obtained by replacing the space derivative with a derivative of arbitrary positive real order $\in (1,2]$, which takes the form of:

$$\rho c\frac{\partial T(x,t)}{\partial t}-k_*\frac{\partial^v T(x,t)}{\partial x^v}+W_b c_b(T(x,t)-T_a)=Q_{ext}+Q_{met},\ t>0,\ 0\leq x\leq R, \tag{1}$$

where $\rho, c, k_*, T, t, x, T_a$, $W_b=\rho_b w_b$, Q_{ext} and Q_{met} symbolize density, specific heat, thermal conductivity, temperature, time, distance, artillery temperature ,blood perfusion rate, metabolic heat generation in skin tissue, and external heat exporter in skin tissue, respectively. The units and values of the symbols expressed in this equation are demonstrated in table 10.

Table 1-The units and values of the symbols expressed in the space-fractional bioheat equation.

Symbol	$\boldsymbol{T_a}$	$\boldsymbol{\rho}$ **and** $\boldsymbol{\rho_b}$	$\boldsymbol{c}$ **and** $\boldsymbol{c_b}$	$\boldsymbol{k_*}$	$\boldsymbol{\omega_b}$	$\boldsymbol{Q_{met}}$
Unit	°C	kg/m^3	J/kg°C	W/m°C	m^3/s/ m^3	W/m^3
value	37	1000	4000	0.5	0.0005	420

The initial and boundary conditions are

$$T(x,0)=T_c, \tag{2}$$

$$-k_*\frac{\partial T}{\partial x}\bigg|_{x=0}=q_0, \tag{3}$$

$$-k_*\frac{\partial T}{\partial x}\bigg|_{x=R}=0. \tag{4}$$

where, q_0 is the heat flux on the skin surface.

3. Preliminaries and Notations

In this section, we recall the essential principles of the fractional calculus theory that will be used in this article.

Definition 1 The Riemann-Liouville fractional integral operator of order $\alpha>0$ is defined as follows [19, 20]:

$$I^\alpha T(x)=\frac{1}{\Gamma(\alpha)}\int_0^x (x-s)^{\alpha-1}\,T(s)ds,\ \ \alpha>0, \qquad I^0\,T(x)=T(x) \tag{5}$$

Definition 2 The Riemann-Liouville definition of fractional differential operator is given as follows [21]:

$$D^\alpha T(x)=\begin{cases}\dfrac{1}{\Gamma(n-\alpha)}\dfrac{d^n}{dt^n}\displaystyle\int_0^x\frac{T(s)}{(x-s)^{\alpha-n+1}}\,ds, \alpha>0, n-1\leq\alpha<n,\\ \dfrac{d^nT(x)}{dx^n} \qquad ,\alpha=n.\end{cases} \tag{6}$$

Definition 3 The Caputo definition of fractional differential operator is defined as below [22]:

$$D^{\alpha}T(x) = \begin{cases} \frac{1}{\Gamma(n-\alpha)} \int_0^x \frac{T^{(n)}(s)}{(x-s)^{\alpha-n+1}} ds, & n-1 \le \alpha < n, \\ \frac{d^n T(x)}{dx^n} & , \alpha = n. \end{cases} \quad (7)$$

The relation between the Riemann-Liouville operator and Caputo operator is given by the following expressions [23]:

$$D^{\alpha} I^{\alpha}\ T(x) = T(x),$$

$$I^{\alpha} D^{\alpha}\ T(x) = T(x) - \sum_{k=0}^{n-1} T^{(k)}(0^+) \frac{x^k}{k!} \quad (8)$$

For $\alpha \ge 0$, $v \ge -1$, and the constant C, Caputo fractional derivative has some basic properties which are needed here, as follows [24]:

$i)\ \ D^{\alpha} C = 0,$

$$ii)\ D^{\alpha} x^{v} = \begin{cases} 0 & \text{for } v \in \mathbb{N}_0 \text{ and } v < \lceil \alpha \rceil \\ \frac{\Gamma(v+1)}{\Gamma(v+1-\alpha)} x^{v-\alpha}, & \text{for } v \in \mathbb{N}_0 \text{ and } v \ge \lceil \alpha \rceil \end{cases} \quad (9)$$

$$iii)\ D^{\alpha}\left(\sum_{i=0}^{n} c_i T_i(x)\right) = \sum_{i=0}^{n} c_i D^{\alpha} T_i(x), \text{ where } \{c_i\}_{i=0}^{n} \text{ are constants}$$

Definition 4 (generalized Taylor's formula). Suppose that $D^{i\alpha}T(x) \in C[0,1]$ for $i = 0(1)(n-1)$, then one has

$$T(x) = \sum_{i=0}^{n-1} \frac{x^{i\alpha}}{\Gamma(i\alpha+1)} D^{i\alpha}T(0^+) + \frac{x^{n\alpha}}{\Gamma(n\alpha+1)} D^{n\alpha}T(\xi) \quad (10)$$

where $0 < \xi \le x, \forall x \in [0,R]$. Also, one has

$$\left| T(x) - \sum_{i=0}^{n-1} \frac{x^{i\alpha}}{\Gamma(i\alpha+1)} D^{i\alpha}T(0^+) \right| \le M_{\alpha} \frac{x^{n\alpha}}{\Gamma(n\alpha+1)} \quad (12)$$

and $M_{\alpha} \ge |D^{n\alpha}T(\xi)|$.

In case $\alpha = 1$, the generalized Taylor's formula (10) is the classical Taylors formula [25].

4. Fractional Shifted Legendre Polynomials

Define the FSLPs by introducing the change of variable $x = x^{\alpha}$ and $n-1 < \alpha \le n$ on shifted Legendre polynomials. The FSLPs $L_n(x^{\alpha})$ is symbolized by $Fl_i^{\alpha}(x)$. The FSLPs are a particular solution of normalized eigenfunctions of the singular Sturm-Liouville problem [21].

$$\left((x - x^{1+\alpha}) Fl_i^{\alpha}(x)\right)' + \alpha^2\, i(i+1) x^{\alpha-1} Fl_i^{\alpha}(x) = 0, \qquad x \in [0,1]. \quad (13)$$

Then $Fl_i^{\alpha}(x)$ can be obtained as follows:

$$Fl_{i+1}^{\alpha}(x) = \frac{(2i+1)(2x^{\alpha}-1)}{i+1} Fl_i^{\alpha}(x) - \frac{i}{i+1} Fl_{i-1}^{\alpha}(x), i = 1,2,\ldots \quad (14)$$

We can derive the analytic form of $Fl_i^{\alpha}(x)$ of degree $i\alpha$ as follows:

$$Fl_i^{\alpha}(x) = \sum_{s=0}^{i} b_{si}\ x^{s\alpha}, \quad (15)$$

where $b_{si} = \frac{(-1)^{i+s}(i+s)!}{(i-s)!(s!)^2}$ and $Fl_i^{\alpha}(0) = (-1)^i$, $Fl_i^{\alpha}(1) = 1$.

Theorem 1 If FSLPs are orthogonal with the weight function $\omega_l^{\alpha}(x) = x^{\alpha-1}$ on the interval [0,1], then the orthogonal condition is

$$\int_0^1 Fl_n^{\alpha}(x)\, Fl_m^{\alpha}(x)\, \omega_l^{\alpha}(x)\, dx = \frac{1}{(2n+1)\alpha} \delta_{nm} \quad (16)$$

Proof. With $\int_0^1 L_n(x)\, L_m(x)\, \omega_l(x) dx = \frac{1}{(2n+1)} \delta_{nm}$, where δ_{nm} is the Kronecker function and the weight function $\omega_l(x) = 1$, let $x = x^{\alpha}$, then we have

$$\int_0^1 L_n(x)\, L_m(x)\, \omega_l(x) dx = \int_0^1 L_n(x^{\alpha})\, L_m(x^{\alpha})\, \alpha x^{\alpha-1}\, dx$$

$$= \frac{1}{(2n+1)} \delta_{nm},$$

$$\int_0^1 L_n(x^\alpha)\, L_m(x^\alpha)\, \alpha x^{\alpha-1}\, dx = \int_0^1 Fl_n^\alpha(x)\, Fl_m^\alpha(x)\ \alpha x^{\alpha-1}\, dx$$

$$= \frac{1}{(2n+1)} \delta_{nm}, \tag{17}$$

$$\int_0^1 Fl_n^\alpha(x)\, Fl_m^\alpha(x)\ x^{\alpha-1}\, dx = \frac{1}{(2n+1)\alpha} \delta_{nm}.$$

Then the theorem is proved.

A temperature function $T(x)$ square integrable in region $0 \le x \le 1$ can be expressed in terms of FSLPs as

$$T(x) = \sum_{i=0}^{\infty} c_i\, Fl_i^\alpha(x) \tag{18}$$

where the coefficients c_i are obtained by

$$c_i = \alpha(2i+1) \int_0^1 Fl_i^\alpha(x) T(x)\, \omega_l^\alpha\,(x) dx, \qquad i = 0,1,2,\ldots \tag{19}$$

Consider a truncated series when $(n+1)$-term FSLPs in (18), then we get

$$T(x) \approx T_n(x) = \sum_{i=0}^{n} c_i\, Fl_i^\alpha(x) = C'\emptyset(x) \tag{20}$$

where the fractional shifted Legendre coefficient vectors C and $\emptyset(x)$ are given by
$C' = [c_0, c_1, \ldots, c_n]$, $\emptyset(x) = [Fl_0^\alpha(x), Fl_1^\alpha(x), \ldots, Fl_n^\alpha(x)]'$.

Theorem 2. Suppose that $D^{i\alpha}T(x) \in C[0,1]$ for $i = 0(1)n$, $(2n+1)\alpha \ge 1$ and $\boldsymbol{P}_n^\alpha = span\{Fl_0^\alpha(x), Fl_1^\alpha(x), \ldots, Fl_n^\alpha(x)\}$. If $T_n(x) = C'\emptyset(x)$ is the best approximation to $T(x)$ from $\boldsymbol{P}_n^\alpha$, then the error bound is presented as follows:

$$\|T(x) - T_n(x)\|_\omega$$

$$\le \frac{M_\alpha}{\Gamma(n\alpha+1)} \sqrt{\frac{1}{(2n+1)\alpha}}\ , \tag{21}$$

where $M_\alpha \ge |D^{n\alpha}T(x)|$, $x \in [0,1]$.

Proof. Consider the generalized Taylor's formula

$$T\,(x) = \sum_{i=0}^{n} \frac{x^{i\alpha}}{\Gamma\,(i\alpha\ +\ 1)} D^{i\alpha}T(0^+) + \frac{x^{n\alpha}}{\Gamma(n\alpha\ +\ 1)} D^{n\alpha}T\,(\xi) \tag{22}$$

where $0\ <\ \xi\ \le\ x$, $\forall x \in [0, 1]$. Also, one has

$$\left| T\,(x) - \sum_{i=0}^{n} \frac{t^{i\alpha}}{\Gamma\,(i\alpha\ +\ 1)} D^{i\alpha} f(0^+) \right| \le M_\alpha\ \frac{x^{n\alpha}}{\Gamma(n\alpha\ +\ 1)} \tag{23}$$

Since $T_n(x) = C'\emptyset(x)$ is the best approximation to $T(x)$ from $\boldsymbol{P}_n^\alpha$ and $\sum_{i=0}^{n} \left(\frac{x^{i\alpha}}{\Gamma(i\alpha+1)}\right) D^{i\alpha} f(0^+) \epsilon\, \boldsymbol{P}_n^\alpha$, hence

$$\|T(x) - T_n(x)\|_\omega^2 \le \left\| T(x) - \sum_{i=0}^{n} \frac{x^{i\alpha}}{\Gamma\,(i\alpha\ +\ 1)} D^{i\alpha}T(0^+) \right\|_\omega^2$$

$$\le \frac{M_\alpha^2}{\left(\Gamma(n\alpha\ +\ 1)\right)^2} \int_0^1 x^{2n\alpha}\, x^{\alpha-1} dx, \tag{24}$$

$$\le \frac{M_\alpha^2}{\left(\Gamma(n\alpha\ +\ 1)\right)^2 (2n+1)\alpha}$$

Now, by taking the square roots both sides, the theorem is proved.
A temperature function $T(x,t) \in L^2([0,1] \times [0,1])$ can be expanded as in the following equation:

$$T(x,t) = \sum_{i=0}^{\infty}\sum_{j=0}^{\infty} c_{ij}\, Fl_i^{\alpha}(x)L_j(t) \tag{25}$$

where

$$c_{ij} = (2i+1)(2j+1)\alpha \int_0^1\int_0^1 T(x,t)\, Fl_i^{\alpha}(x)L_j(t)\omega_l^{\alpha}(x)dxdt, \qquad i,j = 0,1,\dots \tag{26}$$

Theorem3. If the series $\sum_{i=0}^{\infty}\sum_{j=0}^{\infty} c_{ij}\, Fl_i^{\alpha}(x)L_j(t)$ converges uniformly to $T(x,t)$ on the square $[0,1] \times [0,1]$, then we obtain the equation (26).

Proof. By multiplying $\omega_l^{\alpha}(x)Fl_n^{\alpha}(x)L_m(t)$ on both sides of (25), where i and j are fixed and integrating term-wise with regard to x and t on $[0,1] \times [0,1]$, then

$$\begin{aligned}\int_0^1\int_0^1 T(x,t)\, Fl_n^{\alpha}(x)L_m(t)\omega_l^{\alpha}(x)dxdt &= \sum_{i=0}^{\infty}\sum_{j=0}^{\infty} c_{ij}\int_0^1\int_0^1 Fl_i^{\alpha}(x)L_j(t)Fl_n^{\alpha}(x)L_m(t)\omega_l^{\alpha}(x)dxdt\\ &= \textstyle\sum_{i=0}^{\infty}\sum_{j=0}^{\infty} c_{ij}\int_0^1 \omega_l^{\alpha}(x)\, Fl_i^{\alpha}(x)Fl_n^{\alpha}(x)dx \int_0^1 L_j(t)L_m(t)\, dt\\ &= c_{ij}\textstyle\int_0^1 \omega_l^{\alpha}(x)\,[Fl_i^{\alpha}(x)]^2 dx \int_0^1 [L_j(t)]^2\, dt \qquad (27)\\ &= c_{ij}\frac{1}{(2i+1)\alpha}\,\frac{1}{(2j+1)}\end{aligned}$$

Theorem4. If the function $T(x,t)$ is a continuous function on $[0,1] \times [0,1]$ and the series $FL = \sum_{i=0}^{\infty}\sum_{j=0}^{\infty} c_{ij}\, Fl_i^{\alpha}(x)L_j(t)$ converges uniformly to $T(x,t)$, then FL is the FSLPs expansion of $T(x,t)$.

Proof. Using the contradiction, let

$$\left.\begin{aligned}T(x,t) &= \sum_{i=0}^{\infty}\sum_{j=0}^{\infty} c_{ij}\, Fl_i^{\alpha}(x)L_j(t),\\ T(x,t) &= \sum_{i=0}^{\infty}\sum_{j=0}^{\infty} g_{ij}\, Fl_i^{\alpha}(x)L_j(t).\end{aligned}\right\} \tag{28}$$

Then there is at least one coefficient such that $c_{nm} \neq g_{nm}$, however

$$c_{nm} = (2n+1)(2m+1)\alpha\int_0^1\int_0^1 T(x,t)\, Fl_n^{\alpha}(x)L_m(t)\omega_l^{\alpha}(x)dxdt = g_{nm}$$

Theorem 5. If the two continuous functions defined on $[0,1] \times [0,1]$ have the identical FSLPs expansions, then these two function are identical.

Proof. Suppose that $T(x,t)$ and $f(x,t)$ can be expended by FSLPs as follows:

$$T(x,t) \approx \sum_{i=0}^{\infty}\sum_{j=0}^{\infty} c_{ij}\, Fl_i^{\alpha}(x)L_j(t), \tag{29}$$

$$f(x,t) \approx \sum_{i=0}^{\infty}\sum_{j=0}^{\infty} c_{ij}\, Fl_i^{\alpha}(x)L_j(t). \tag{30}$$

By subtracting equation (30) from (29), we obtain

$$T(x,t) - f(x,t) \approx \textstyle\sum_{i=0}^{\infty}\sum_{j=0}^{\infty}\left(c_{ij} - c_{ij}\right) Fl_i^{\alpha}(x)L_j(t) = 0 \tag{31}$$

Theorem 6. If the sum of the absolute values of the FSLPs coefficients of a continuous function $T(x,t)$ forms a convergent series, then the FSLPs expansion is absolutely uniformly convergent and converges to the function $T(x,t)$.
Proof. Consider that

$$\left|\sum_{i=0}^{\infty}\sum_{j=0}^{\infty} c_{ij}\, Fl_i^{\alpha}(x)L_j(t)\right| \le \sum_{i=0}^{\infty}\sum_{j=0}^{\infty}\left|c_{ij}\right| \left|Fl_i^{\alpha}(x)\right|\left|L_j(t)\right|$$
$$\le \sum_{i=0}^{\infty}\sum_{j=0}^{\infty}\left|c_{ij}\right| \qquad (32)$$

Suppose a truncated series in (25), which satisfies

$$T(x,t) \approx \sum_{i=0}^{n}\sum_{j=0}^{m} c_{ij}\, Fl_i^{\alpha}(x)L_j(t)$$
$$= \emptyset'(x)C\emptyset(t), \qquad (33)$$

where

$\emptyset(x) = [Fl_0^{\alpha}(x), Fl_1^{\alpha}(x), \dots, Fl_n^{\alpha}(x)]'$; $\emptyset(t) = [L_0(t), L_1(t), \dots, L_m(t)]'$ and $C = \{c_{ij}\}_{i,j=0}^{n,m}$.

5. Two-Dimensional Fractional Shifted Legendre Operational Matrix of Fractional Differentiation

The derivative of the $\emptyset(x)$ can be approximated as follows

$$\emptyset^{(v)}(x) \approx D^{v}\emptyset(x), \qquad (34)$$

where D^{v} is called the FSLPs in the matrix of space derivative.

Theorem 7. Suppose that the Caputo fractional derivative D^{v} is $(m+1)\times(m+1)$ matrix of order $v > 0, \alpha > \frac{v}{2}$, when $\alpha \notin \mathbb{N}$, which have the elements defined by

$$\{d_{ij}\}_{i,j=0}^{m,m} = \alpha(2j+1)\sum_{s=0}^{i}\sum_{r=0}^{j} b_{rj}\, b'_{si}\frac{\Gamma(s\alpha+1)}{\Gamma(s\alpha - v+1)((s+r+1)\alpha - v)} \qquad (35)$$

where

$$b'_{si} = \begin{cases} 0, & s\alpha \in \mathbb{N}_0,\ \ s\alpha < v, \\ b'_{si} = b_{si} & s\alpha \notin \mathbb{N}_0, s\alpha \ge \lceil v \rceil\ or\ s\alpha \in \mathbb{N}_0, s\alpha \ge v. \end{cases} \qquad (36)$$

Proof. From the property (ii) of equation (9) and the orthogonally of FSLPs, we get

$$D^{v}Fl_i^{\alpha}(x) = \sum_{s=0}^{i} b'_{si}\frac{\Gamma(s\alpha+1)}{\Gamma(s\alpha - v+1)}\, x^{s\alpha - v}, \qquad (37)$$

let

$$x^{s\alpha - v} = \sum_{j=0}^{m} d_j\, Fl_j^{\alpha}(x) \qquad (38)$$

By multiplying both sides of the equation (38) by $\omega_l^{\alpha}(x)Fl_j^{\alpha}(x)$, it yields

$$d_i = (2i+1)\alpha \sum_{r=0}^{j} b_{rj}\,\frac{1}{(s+r+1)\alpha - v}, \qquad (39)$$

By substituting the equations (38) and (39) into equation (37), we have

$$D^{v}Fl_i^{\alpha}(x) = (2j+1)\alpha\sum_{j=0}^{m}\sum_{s=0}^{i}\sum_{r=0}^{j} b_{rj}b'_{si}\frac{\Gamma(s\alpha+1)}{\Gamma(s\alpha - v+1)((s+r+1)\alpha - v)}\, Fl_j^{\alpha}(x), \qquad (40)$$

hence,

$$d_{ij} = \alpha(2j+1)\sum_{s=0}^{i}\sum_{r=0}^{j} b_{rj}\, b'_{si}\frac{\Gamma(s\alpha+1)}{\Gamma(s\alpha - v+1)((s+r+1)\alpha - v)} \qquad i,j = 0(1)\,m \qquad (41)$$

6. Method for the Solution

Now, we will structure the approximate solution of equation (1) under given conditions, as in the following series form

$$T(x,t)=\sum_{i=0}^{\infty}\sum_{j=0}^{\infty} t_{ij}\, Fl_i^{\alpha}(x)L_i(t) \tag{42}$$

which is equivalent to the matrix form

$$T(x,t)=\emptyset'(x)T\emptyset(t) \tag{43}$$

where

$T=\{t_{ij}\}_{i,j=0}^{n,m}$, $\emptyset(t)=[L_0(t),L_1(t),\dots,L_m(t)]'$, $\emptyset(x)=[Fl_0^{\alpha}(x),Fl_1^{\alpha}(x),\dots,Fl_n^{\alpha}(x)]'$

The approximate of the first temporal and spatial derivatives can be written as

$$\frac{\partial T(x,t)}{\partial t}=\emptyset'(x)\,TD_t\emptyset(t) \tag{44}$$

$$\frac{\partial T(x,t)}{\partial x}=\emptyset'(x)(D_x)'\,T\emptyset(t) \tag{45}$$

and the fractional spatial derivative as

$$\frac{\partial^{v} T(x,t)}{\partial x^{v}}=\emptyset'(x)(D_x^{v})'\,T\emptyset(t) \tag{46}$$

By applying the solution method for S-FBHE in (1), we have

$$\rho c\,\emptyset'(x)TD_t\emptyset(t)-k_*\emptyset'(x)(D_x^{v})'T\emptyset(t)+W_bc_b\emptyset'(x)T\emptyset(t)$$
$$=\emptyset'(x)Q_{ext}\emptyset(t)+\emptyset'(x)Q_{met}\emptyset(t)+\emptyset'(x)W_bc_bT_a\emptyset(t), \tag{47}$$

where

$g(x,t)=Q_{ext}+Q_{met}+W_bc_bT_a$

$\emptyset'(x)G\,\emptyset(t)=\emptyset'(x)Q_1\emptyset(t)+\emptyset'(x)Q_2\emptyset(t)+\emptyset'(x)Q_3\emptyset(t)$

$G=Q_1+Q_2+Q_3$

$\emptyset'(x)G\,\emptyset(t)=\emptyset'(x)Q_1\emptyset(t)+\emptyset'(x)Q_2\emptyset(t)+\emptyset'(x)Q_3\emptyset(t)andG=\{g_{ij}\}_{i,j=0}^{n,m}$,

$$g_{ij}=\alpha(2i+1)(2j+1)\int_0^1\int_0^1 g(x,t)\,Fl_i^{\alpha}(x)L_j(t)\omega_l^{\alpha}(x)dxdt \tag{48}$$

Multiplying by $\omega_l^{\alpha}(x)Fl_i^{\alpha}(x)L_j(t)$ generates $mn+n+m+1$ algebraic equations for $i=0(1)(n)$, $j=0(1)m$. Then, by integrating from 0 to 1 and using the orthogonal property, we have

$$T(\rho c\,D_t-\omega_b\rho_bc_bI)-k_*(D_x^{v})'T=G, \tag{49}$$

with the initial condition from equation (2) in the matrix form is as follows:

$$T\emptyset(0)\approx F \tag{50}$$

where

$F=[f_0,f_1,\dots,f_m]'$

$$f_j=\alpha(2j+1)\int_0^1 T(x,0)\,Fl_j^{\alpha}(x)\omega_l^{\alpha}(x)dx \tag{51}$$

and the boundary conditions from equations (3) and (4), respectively, in the matrix form give

$$-k_*\emptyset'(0)D_x{}'T\approx K' \tag{52}$$

$$-k_*\emptyset'(R)D_x{}'T\approx H' \tag{53}$$

where

$K=[k_0\quad k_1\quad \cdots\ k_n]'$ and $H=[h_0\quad h_1\quad \cdots\ h_n]'$

$$k_i=(2i+1)\int_0^1 T_x(0,t)\,L_i(t)\omega_l(t)dt, \tag{54}$$

$$h_i=(2i+1)\int_0^1 T_x(R,t)\,L_i(t)\omega_l(t)dt \tag{55}$$

which generates the $nm+n+m+1$ linear algebraic equations by equation (49) together with equations (50),(52) and (53). These unknown coefficients T can be found by solving Sylvester system.

7. Error Analysis

Consider $e(x,t) = T(x,t) - T_{nm}(x,t)$ as the error function where $T_{nm}(x,t)$ and $T(x,t)$ are the approximate solution and the theoretical solution of (1), respectively.
Therefore, $T_{nm}(x,t)$ satisfies the following problem

$$\rho c \frac{\partial T_{nm}(x,t)}{\partial t} - k_* \frac{\partial^v T_{nm}(x,t)}{\partial x^v} + W_b c_b T_{nm}(x,t) + R_{nm}(x,t) = g(x,t), \tag{56}$$

where $R_{nm}(x,t)$ is the residual function,

$$R_{nm}(x,t) = \rho c \frac{\partial T_{nm}(x,t)}{\partial t} - k_* \frac{\partial^v T_{nm}(x,t)}{\partial x^v} + W_b c_b T_{nm}(x,t) - g(x,t). \tag{57}$$

We can find an approximation $\tilde{e}_{nm}(x,t)$ to the error function $e_{nm}(x,t)$ using the same procedure as the previous one. Thus, the error function satisfies the solution of the equation

$$\rho c \frac{\partial e_{nm}(x,t)}{\partial t} - k_* \frac{\partial^v e_{nm}(x,t)}{\partial x^v} + W_b c_b e_{nm}(x,t) = R_{nm}(x,t). \tag{58}$$

We should note that in order to construct the approximate $\tilde{e}_{nm}(x,t)$ to the error function $e_{nm}(x,t)$, only equation (58) needs to be recalculated by using the same procedure used for solution (1).

8. Numerical Experiments

In order to show the ability of the collocation method to achieve the high accuracy, we utilize now the proposed method presented in this article for two examples, in which the collocation method is implemented for solving the S-FBHE based on FSLPs. In these examples, the solution obtained from this method is compared with the exact solution using the computer device Asus Core i5 (2012) and MATLAB R2018a software.

The S-FBHE is transformed into the linear algebraic equations $(49), (50), (52)$ and (53) respectively. In these examples, take $v = \alpha$, $R = 1$ and use evenly-spaced grid points. Tables 2-7 shows the absolute errors obtained from solving the S-FBHE using FSLPs, for different fractional order $\alpha = 1.51, 1.7, 1.9$ at $t = 1, 1.2, 1.3$ and $x \in [0, R]$ for different values of order $n = m = 6(2)12$.

Example1

Consider the S-FBHE (1) with choosing Q_{ext}, so the exact solution is:

$$T(x,t) = e^{-x} t^{1+\alpha} + 37 \tag{59}$$

with the initial condition

$$T(x,0) = 37, \quad x \in [0,R] \tag{60}$$

and the boundary conditions

$$-k_* \frac{\partial T(0,t)}{\partial x} = -t^{1+\alpha} \quad , t > 0 \tag{61}$$

$$-k_* \frac{\partial T(R,t)}{\partial x} = -e^{-R} t^{1+\alpha} \quad , t > 0 \tag{62}$$

Table 2- Absolute Errors of Example 1 with $R = 1$ and $\alpha = 1.51$.

$(\boldsymbol{x}, \boldsymbol{t})$	**Absolute error** $\mathbf{n \times m = 6 \times 6}$ **CPU=** $\mathbf{160.329415s}$	**Absolute error** $\mathbf{n \times m = 8 \times 8}$ **CPU=** $\mathbf{283.492145s}$	**Absolute error** $\mathbf{n \times m = 10 \times 10}$ **CPU=** $\mathbf{449.555917s}$	**Absolute error** $\mathbf{n \times m = 12 \times 12}$ **CPU=** $\mathbf{763.665118s}$
(0,0)	9.2897e-05	2.1589e-05	7.3668e-06	3.1496e-06
(0.1,0.1)	1.3553e-04	6.6216e-05	2.6084e-05	9.0596e-06
(0.2,0.2)	3.5470e-04	3.9097e-05	2.1405e-05	1.2136e-05
(0.3,0.3)	1.7135e-04	1.0657e-04	3.0567e-06	3.0460e-05
(0.4,0.4)	3.5248e-04	6.8506e-06	7.2961e-05	3.9723e-05
(0.5,0.5)	5.7297e-04	2.4522e-04	9.5092e-05	2.6318e-05
(0.6,0.6)	1.3067e-04	1.3149e-05	9.3588e-06	1.6524e-05
(0.7,0.7)	1.1601e-03	4.1668e-04	1.7085e-04	6.6750e-05
(0.8,0.8)	4.5665e-04	3.3147e-04	2.7213e-04	9.9522e-05
(0.9,0.9)	2.1217e-03	6.0418e-05	3.7764e-04	1.3092e-05
(1,1)	6.0224e-03	2.6419e-03	1.4417e-03	8.9283e-04

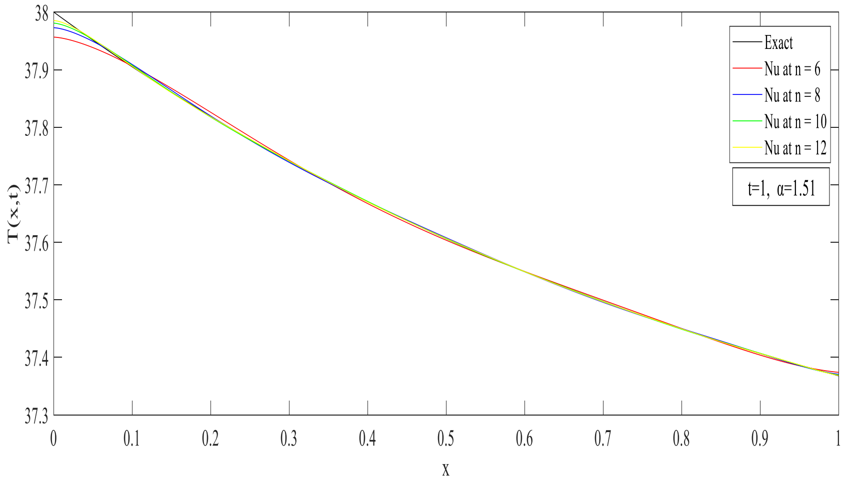

Figure 1- Comparison between exact and numerical solutions for Example 1 at $\alpha = 1.51, , R = 1, n = 6(2)12$.

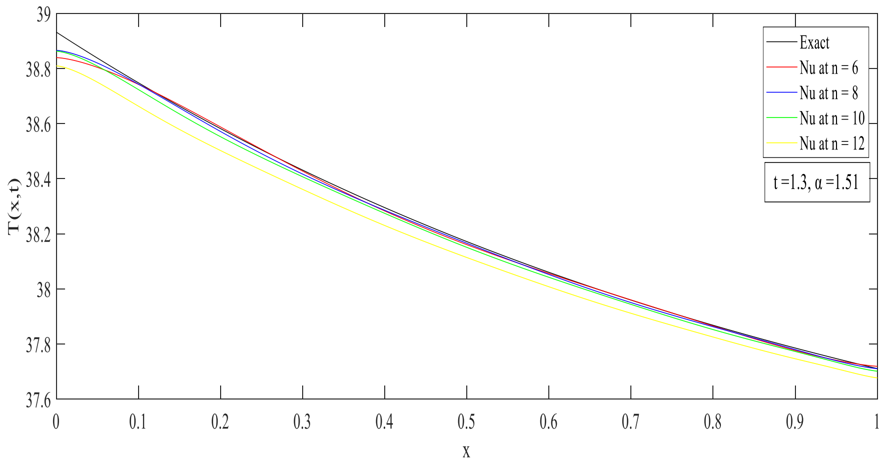

Figure2- Comparison between exact and numerical solutions for Example 1 at $\alpha = 1.51, R = 1, n = 6(2)12$

Table 3- Absolute Errors of Example 1 with $R = 1$ and $\alpha = 1.7$.

$(\boldsymbol{x}, \boldsymbol{t})$	**Absolute error** $\mathbf{n \times m = 6 \times 6}$ **CPU=** $\mathbf{132.424413s}$	**Absolute error** $\mathbf{n \times m = 8 \times 8}$ **CPU=** $\mathbf{236.526092s}$	**Absolute error** $\mathbf{n \times m = 10 \times 10}$ **CPU=** $\mathbf{423.834810s}$	**Absolute error** $\mathbf{n \times m = 12 \times 12}$ **CPU=** $\mathbf{751.131544}\boldsymbol{s}$
(0,0)	1.6367e-04	4.0087e-05	1.4241e-05	6.2724e-06
(0.1,0.1)	7.8288e-06	3.1301e-05	2.0602e-05	1.2090e-05
(0.2,0.2)	3.0937e-04	8.2960e-05	3.4689e-06	2.1882e-05
(0.3,0.3)	3.3061e-04	9.8121e-05	5.4720e-05	2.6801e-05
(0.4,0.4)	2.2588e-04	1.5303e-04	1.0603e-04	2.0960e-06
(0.5,0.5)	8.2192e-04	2.4738e-04	2.4530e-05	5.2812e-05
(0.6,0.6)	3.2032e-04	2.2636e-04	1.6229e-04	1.1473e-04
(0.7,0.7)	1.2352e-03	5.4656e-04	2.8736e-04	1.6718e-04
(0.8,0.8)	1.0918e-03	1.3128e-04	3.1273e-04	2.1998e-04
(0.9,0.9)	1.5044e-03	4.1016e-04	4.7191e-04	1.6846e-04
(1,1)	7.6506e-03	3.6415e-03	2.0928e-03	1.3461e-03

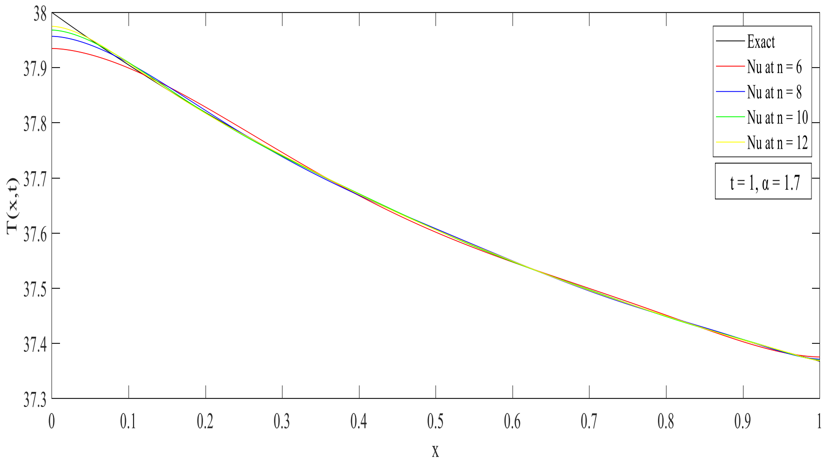

Figure 3- Comparison between exact and numerical solutions for Example 1 at $\alpha = 1.7, R = 1, n = 6(2)12$.

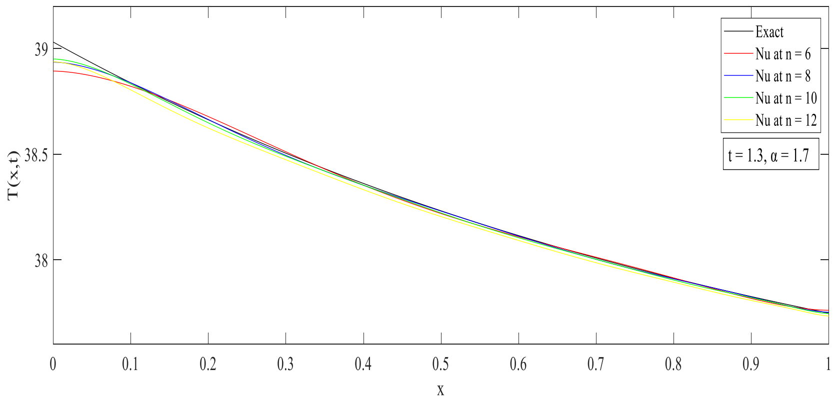

Figure 4- Comparison between exact and numerical solutions for Example 1 at $\alpha = 1.7, R = 1, n = 6(2)12$.

Table 4- Absolute Errors of Example 1 with $R = 1$ and $\alpha = 1.9$.

(x, t)	**Absolute error** $\mathbf{n \times m = 6 \times 6}$ **CPU=** $\mathbf{127.307871s}$	**Absolute error** $\mathbf{n \times m = 8 \times 8}$ **CPU=** $\mathbf{242.393609s}$	**Absolute error** $\mathbf{n \times m = 10 \times 10}$ **CPU=** $\mathbf{439.252672s}$	**Absolute error** $\mathbf{n \times m = 12 \times 12}$ **CPU=** $\mathbf{723.600739s}$
(0,0)	1.2717e-04	3.2815e-05	1.2145e-05	5.5269e-06
(0.1,0.1)	7.3374e-05	5.2176e-06	6.4377e-06	7.8466e-06
(0.2,0.2)	1.5266e-04	8.9358e-05	2.4491e-05	1.0377e-05
(0.3,0.3)	3.7748e-04	2.2417e-05	8.5757e-05	5.1349e-06
(0.4,0.4)	2.8351e-05	2.5296e-04	5.4700e-05	6.7004e-05
(0.5,0.5)	8.1117e-04	9.9161e-05	1.1810e-04	1.1922e-04
(0.6,0.6)	7.9471e-04	4.6563e-04	2.7197e-04	1.4492e-04
(0.7,0.7)	9.7692e-04	4.6138e-04	2.5954e-04	1.6384e-04
(0.8,0.8)	1.7323e-03	2.4698e-04	1.7967e-04	2.4811e-04
(0.9,0.9)	2.5822e-03	8.5326e-04	4.2100e-04	3.5956e-04
(1,1)	9.1330e-03	4.6075e-03	2.7557e-03	1.8270e-03

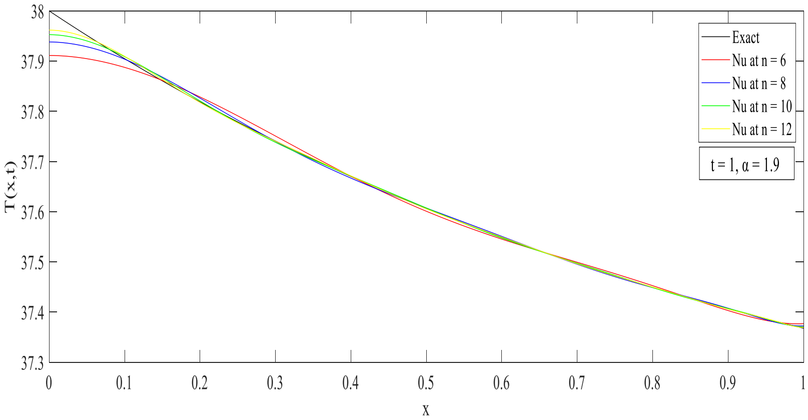

Figure 5- Comparison between exact and numerical solutions for Example 1 at $\alpha = 1.9, R = 1, n = 6(2)12$.

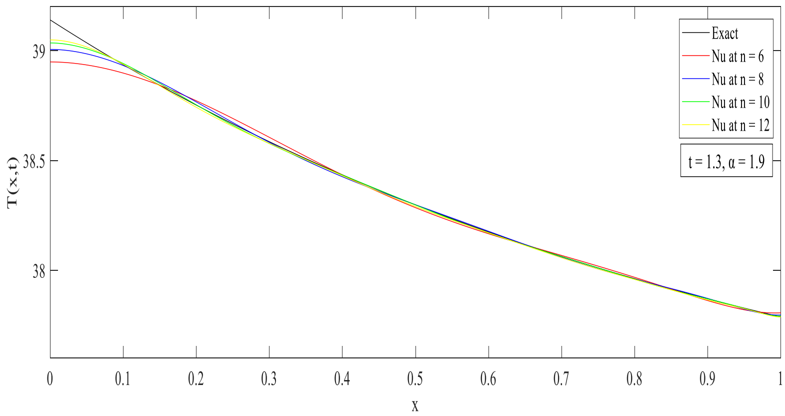

Figure 6- Comparison between exact and numerical solutions for Example 1 at $\alpha = 1.9, R = 1, n = 6(2)12$.

Example 2

Consider the S-FBHE (1) with choosing Q_{ext}, so the exact solution is [8]:

$$T(x,t) = t^{\frac{3}{2}} x^2 \left(\frac{3}{2} - x\right) + 37 \tag{63}$$

with the initial condition

$$T(x,0) = 37, \quad x \in [0,R] \tag{64}$$

and boundary conditions

$$-k_* \frac{\partial T(0,t)}{\partial x} = 0 \ , t > 0 \tag{65}$$

$$-k_* \frac{\partial T(R,t)}{\partial x} = 3t^{\frac{3}{2}} R(1-R) \ , t > 0 \tag{66}$$

Table 5- Absolut Errors Obtained for Example 2 with $R = 1$ and $\alpha = 1.5$.

(x,t)	**Absolute error** $\mathbf{n \times m = 6 \times 6}$ **CPU=** $\mathbf{159.439663s}$	**Absolute error** $\mathbf{n \times m = 8 \times 8}$ **CPU=** $\mathbf{332.868450\ s}$	**Absolute error** $\mathbf{n \times m = 10 \times 10}$ **CPU=**$\mathbf{652.098277}s$	**Absolute error** $\mathbf{n \times m = 12 \times 12}$ **CPU=** $\mathbf{4683.959786}s$
(0,0)	4.7535e-04	2.0206e-04	1.0329e-04	5.9661e-05
(0.1,0.1)	3.8248e-04	2.8583e-04	1.7071e-04	9.0607e-05
(0.2,0.2)	1.1027e-03	3.3929e-04	7.8038e-05	3.7306e-05
(0.3,0.3)	9.1218e-04	9.5409e-05	1.1130e-04	1.0378e-04
(0.4,0.4)	2.3700e-04	1.8279e-04	1.7801e-04	2.9282e-05
(0.5,0.5)	7.9141e-05	3.5798e-04	2.4337e-05	6.9434e-05

(0.6,0.6)	2.9689e-04	1.2515e-04	5.5775e-05	3.2100e-05
(0.7,0.7)	7.1184e-04	1.3955e-04	8.2098e-05	3.3098e-06
(0.8,0.8)	1.1209e-04	5.9892e-05	9.6552e-05	4.8572e-06
(0.9,0.9)	1.1027e-03	1.3805e-04	2.6357e-06	3.5864e-05
(1,1)	1.2685e-03	2.2910e-04	4.4188e-05	7.2284e-07

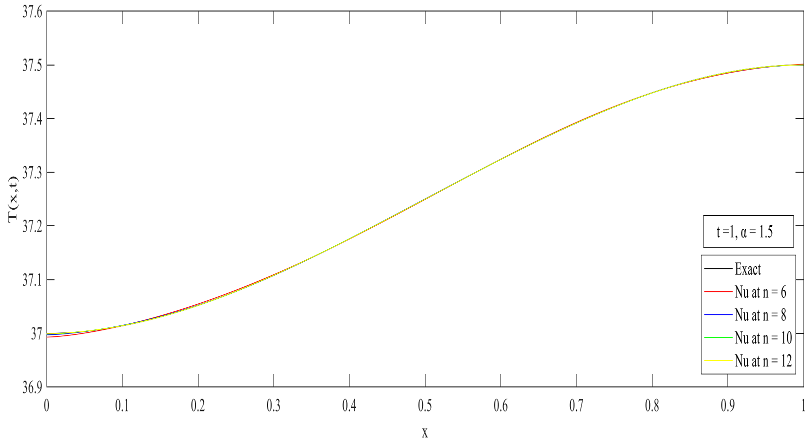

Figure7- Comparison between exact and numerical solutions for Example 2 at $\alpha = 1.5\,, R = 1, n = 6(2)12$.

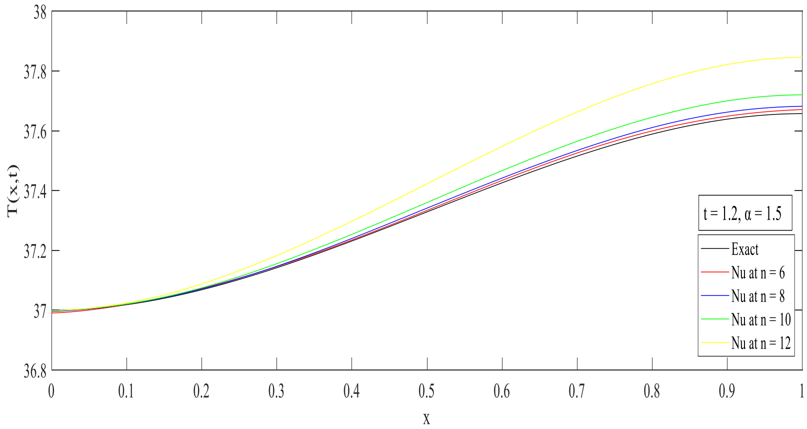

Figure 8- Comparison between exact and numerical solutions for Example 2 at $\alpha = 1.5, R = 1, n = 6(2)12$.

Table 6- Absolute Errors Obtained for Example 2 with $R = 1$ and $\alpha = 1.7$

$(\boldsymbol{x}, \boldsymbol{t})$	**Absolute error** $\mathbf{n \times m = 6 \times 6}$ **CPU=** $\mathbf{152.784115s}$	**Absolute error** $\mathbf{n \times m = 8 \times 8}$ **CPU=** $\mathbf{367.743789s}$	**Absolute error** $\mathbf{n \times m = 10 \times 10}$ **CPU=**$\mathbf{846.523806}\boldsymbol{s}$	**Absolute error** $\mathbf{n \times m = 12 \times 12}$ **CPU=** $\mathbf{20918.601336s}$
(0,0)	8.3083e-04	3.0972e-04	1.4822e-04	8.2125e-05
(0.1,0.1)	1.1516e-04	2.6053e-04	2.1113e-04	1.4459e-04
(0.2,0.2)	1.3158e-03	5.7888e-04	1.8768e-04	5.0078e-05
(0.3,0.3)	1.3977e-03	1.8043e-04	4.4541e-05	9.5541e-05
(0.4,0.4)	4.6102e-04	1.9667e-05	1.9508e-04	6.4368e-05
(0.5,0.5)	3.2579e-04	3.0703e-04	5.6517e-05	1.5953e-05
(0.6,0.6)	1.3631e-04	1.8300e-04	4.4848e-05	5.0623e-05
(0.7,0.7)	4.0343e-04	2.7092e-04	7.3656e-05	5.8390e-05
(0.8,0.8)	1.0396e-04	1.0850e-04	1.6530e-04	2.6468e-06
(0.9,0.9)	1.2614e-03	2.3628e-04	5.8947e-05	8.9319e-05
(1,1)	1.2726e-04	2.4118e-05	4.6645e-06	1.0673e-05

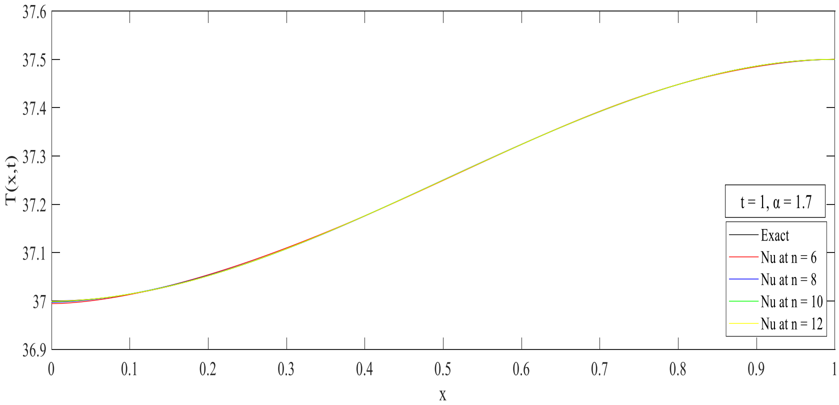

Figure 9- Comparison between exact and numerical solutions for Example 2 at $\alpha = 1.7, R = 1, n = 6(2)12$.

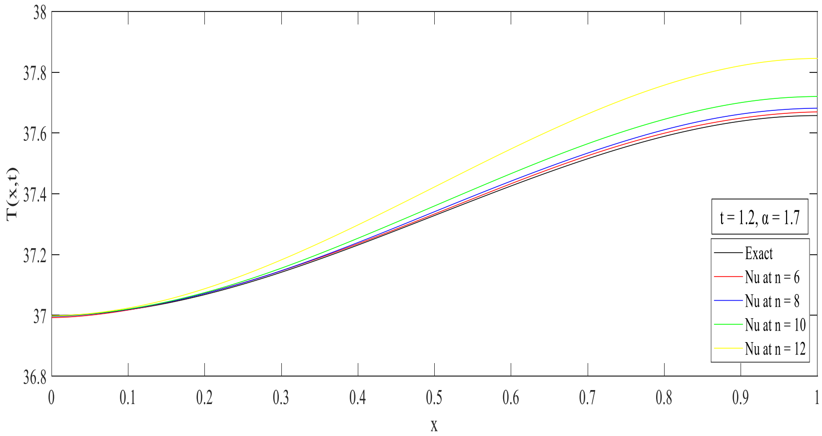

Figure10- Comparison between exact and numerical solutions for Example 2 at $\alpha = 1.7$, $R = 1, n = 6(2)12$.

Table 7- Absolut Errors Obtained for Example 2 with $R = 1$ and $\alpha = 1.9$

(x,t)	**Absolute error** $N \times M = 6 \times 6$ **CPU=** $152.596047s$	**Absolute error** $N \times M = 8 \times 8$ **CPU=** $333.750116s$	**Absolute error** $N \times M = 10 \times 10$ **CPU=** $646.495021s$	**Absolute error** $N \times M = 12 \times 12$ **CPU=** $1173.085625s$
(0,0)	1.6561e-03	5.8557e-04	2.6635e-04	1.4041e-04
(0.1,0.1)	5.2281e-04	9.5436e-05	1.8358e-04	1.6569e-04
(0.2,0.2)	1.3320e-03	8.0221e-04	3.6057e-04	1.2871e-04
(0.3,0.3)	1.9028e-03	3.8942e-04	5.6962e-06	2.4652e-05
(0.4,0.4)	7.5477e-04	1.5740e-04	1.0235e-04	1.0853e-04
(0.5,0.5)	6.1954e-04	1.0970e-04	1.1064e-04	3.5566e-05
(0.6,0.6)	6.4969e-04	1.8860e-04	1.4415e-04	2.8657e-05
(0.7,0.7)	3.8694e-05	3.9736e-04	6.3546e-06	9.7660e-05
(0.8,0.8)	5.7872e-04	2.9104e-04	2.2942e-04	3.6989e-05
(0.9,0.9)	1.5016e-03	4.3705e-04	1.4489e-04	1.4288e-04
(1,1)	2.3591e-03	6.8923e-04	2.7628e-04	1.3131e-04

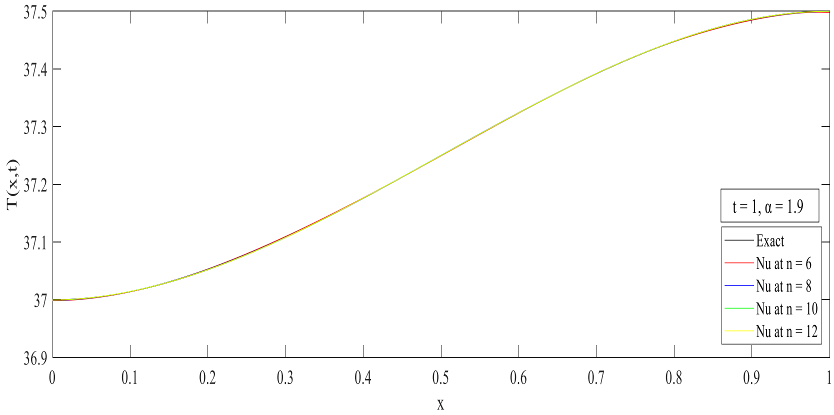

Figure 11- Comparison between exact and numerical solutions for Example 2 at $\alpha = 1.9$, $R = 1$, $n = 6(2)12$

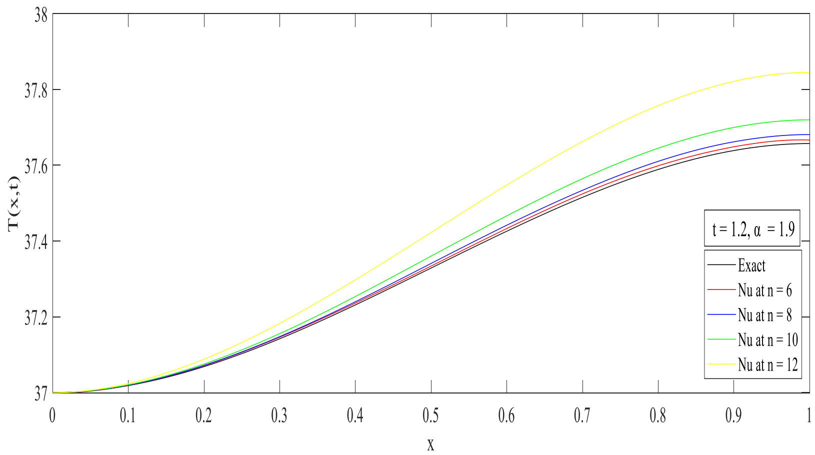

Figure12- Comparison between exact and numerical solutions for Example 2 at $\alpha = 1.9$, $R = 1$, $n = 6(2)12$

9. Conclusions

In this article, the FSLPs were employed in the matrix form to solve S-FBHE successfully. The Caputo formula was utilized to approximate the fractional derivative. The computational outcomes specified that the present methodology has higher accuracy, good convergence, and reasonable stability, as well as a less computation effect by using few grid points.

Figs. 1-12 clarified comparisons between the exact solutions and numerical outcomes of Examples 1 and 2, showing that the FSLPs have high accuracy and good convergence by increasing n. We could also observe the effect of increasing t from the figures.

References

1. Ahmad F., Alomari A., Bataineh A., Sulaiman J. and Hashim I. **2016.** On the approximate solutions of systems of ODEs by Legendre operational matrix of differentiation, *Italian Journal of Pure and Applied Mathematics*, **36**: 483-494.
2. Mishra T., Rai K. **2015.** Implicit finite difference approximation for time Fractional heat conduction under boundary condition of second kind, *International Journal of Applied Mathematical Research*, **4**(1): 135-149.
3. Sarkar N. **2015.** On a new time-fractional order bio-heat transfer model, *International Research Journal of Engineering and Technology (IRJET)*, **2**(4): 1140-1142.
4. Suna H., Zhang Y., Baleanu D., Chen W. and Chen Y **2018.** A new collection of real world applications of fractional calculus in science and engineering, *Communications in Nonlinear Science and Numerical Simulation*, **64**: 213-231.

5. Tohidi E. **2012.** Legendre approximation for solving linear HPDEs and comparison with Taylor and Bernoulli matrix methods, *Applied Mathematics*, **3**: 410-416.

6. Damor R., Kumar S. and Shukla A. **2014**. Numerical simulation of fractional bioheat equation in hyperthermia treatment, *Journal of Mechanics in Medicine and Biology*, **14**(2): 1-15.

7. Damor R., Kumar S. and Shukla A. **2015.** Paramatrac study of fractional bioheat equation in skin tissue with sinusoidal heat flux, *Fractional Differential Calculus*, **5**(1): 43-53.

8. Ferrás L., Ford N., Morgado M., Nobrega J. and Rebelo M. **2015.** Fractional Pennes' bioheat equation: Theoretical and numerical studies, *Fractional Calculus and Applied Analysis*, **18**(4): 1080-1106.

9. Pennes H. **1948.** Analysis of tissue and arterial blood temperature in the resting forearm, *Journal of applied physiology*, **1**: 93-122.

10. Singh J., Gupta P. and Rai K. **2011.** Solution of fractional bioheat equations by finite difference method and HPM, *Mathematical and Computer Modelling*, **54**: 2316-2325.

11. Jiang X. and Qi H., **2012.** Thermal wave model of bioheat transfer with modified Riemann–Liouville fractional derivative, *Journal of Physics A: Mathematical and Theoretical*, **45**: 1-11.

12. Damor R., Kumar S. and Shukla A., **2013.** Numerical solution of fractional bioheat equation with constant and sinusoidal heat flux condition on skin tissue, *American Journal of Mathematical Analysis*, **1**(2): 20-24.

13. Ezzat M., AlSowayan N., Al-Muhiameed Z. and Ezzat S. **2014.** Fractional modelling of Pennes' bioheat transfer equation, *Heat and Mass Transfer*, **50**(7): 907-914.

14. Kumar P., Kumar D. and Rai K., **2015.** A mathematical model for hyperbolic space-fractional bioheat transfer during thermal therapy, *Procedia Engineering*, **127**: 56-62.

15. Qin Y. and Wu K. **2016.** Numerical solution of fractional bioheat equation by quadratic spline collocation method, *Journal of Nonlinear Science and Applications*, **9**: 5061-5072.

16. Kumar D. and Rai K. **2017.** Numerical simulation of time fractional dual-phase-lag model of heat transfer within skin tissue during thermal therapy, *Journal of Thermal Biology*, **67**: 49-58.

17. Roohi R., Heydari M., Aslami M., and Mahmoudi M. **2018.** A comprehensive numerical study of space-time fractional bioheat equation using fractional-order Legendre functions, *The European Physical Journal Plus*, **133**(412): 1-15.

18. Hosseininia M., Heydari M., Roohi R. and Avazzadeh Z. **2019.** A computational wavelet method for variable-order fractional model of dual phase lag bioheat equation, **395**: 1-18.

19. Dehghan M. and Sabouri M., **2012.** A spectral element method for solving the Pennes bioheat transfer equation by using triangular and quadrilateral elements, *Applied Mathematical Modelling*, **36**: 6031–6049(2012).

20. Chen Y., Sun Y. and Liu L. **2014.** Numerical solution of fractional partial differential equations with variable coefficients using generalized fractional-order Legendre functions, *Applied Mathematics and Computation*, **244**: 847-858.

21. Huang Q., Zhao F., Xie J., Ma L., Wang J. and Li Y. **2017.** Numerical approach based on two-dimensional fractional-order Legendre functions for solving fractional differential equations, *Discrete Dynamics in Nature and Society*, 1-12.

22. Abdeljawad T. **2011.** On Riemann and Caputo fractional differences, *Computers and Mathematics with applications*, **62**: 1602-1611.

23. Abdo M., Panchal S. and Saeed A. **2019**. Fractional boundary value problem with ψ-Caputo fractional derivative, *Proc. Indian Acad. Sci. (Math. Sci.)*, **129**(65): 1-14.

24. Ishteva M. **2005**. Properties and applications of the Caputo fractional operator, M.Sc.Thesis, Department of mathematics, University Karlsruhe (TH), Sofia (Bulgaria).

25. Odibat M. and Shawagfeh N. **2007**. Generalized Taylor's formula, *Applied Mathematics and Computation*, **186**: 286-293.